Thermal Characterization of Kraft Lignin Prepared from Mixed Hardwoods

Justin Alfred Pe III,[a] Ji Sun Mun,[b] and Sung Phil Mun [a,*]

Thermal characterization of kraft lignin (KL) prepared from mixed hardwoods was conducted to determine their thermal and thermo-oxidative stability, glass transition temperature (T_g), pyrolysis products composition, and syringyl/guaiacyl ratio. Two milled wood lignins (MWLs) from acacia (MWL-aca) and mixed hardwoods (MWL-mhw), the same hardwood species employed in the production of KL, were also characterized for comparison with KL. Thermogravimetric analysis (TGA) indicated that KL had higher thermal and thermo-oxidative stability than MWLs. Based on differential scanning calorimetry (DSC), the T_g of KL was 63.2 °C, while MWLs gave similar values near 165 °C. The syringyl (S), guaiacyl (G), *p*-hydroxyphenyl (H) composition of KL acquired from pyrolysis-gas chromatography/mass spectrometry (Py-GC/MS) at 675 °C was 48:44:8 (S/G ratio 1.07), while MWL-aca and MWL-mhw were 31:60:9 and 46:48:6, respectively.

DOI: 10.15376/biores.18.1.926-936

Keywords: Kraft lignin (KL); Acacia; Mixed hardwoods; Thermal analysis; Pyrolysis-GC/MS; Syringyl (S); Guaiacyl (G)

*Contact information: a: Department of Wood Science and Technology, Jeonbuk National University, Jeonju, 54896 South Korea; b: Department of Carbon Materials and Fiber Engineering, Jeonbuk National University, Jeonju, 54896 South Korea; *Corresponding author: msp@jbnu.ac.kr*

INTRODUCTION

Lignin is the second most abundant bioresource next to cellulose and is the major source of aromatic compounds in nature. Lignin has mainly been produced from the pulp and paper industries. Approximately 50 million tons of kraft lignin (KL) are produced worldwide per year, of which about 98 to 99% are incinerated to generate steam or energy (Demuner *et al*. 2019). In 2019, Moorim P&P, South Korea's only kraft pulping mill, produced 450,000 tons of pulp, and the resulting black liquor was utilized as fuel to recover its pulping chemicals and energy content. In reality, only a fraction of these KLs are used to make value-added products; this limited utilization of KLs is due to their poor solubility in water, structural complexity, and heterogeneity. Chemical or thermal modifications have been performed to overcome these limitations and to increase KL's reactivity and processability. Some examples of value-added products derived from KL, which underwent modifications, were carbon fibers (Kadla *et al*. 2002; Bengtsson *et al*. 2020), bio-aviation fuels (Kim *et al*. 2020), and KL-based polypropylene (PP) (Chen *et al*. 2011) and poly(lactic) acid (PLA) blends (Gordobil *et al*. 2014, 2015). Chen *et al*. (2011) worked on the alkylation of KL using bromododecane to improve the compatibility of PP and KL. Interestingly, addition of 5% alkylated KL to PP increased the thermal stability by about 27 °C with respect to pure PP. Moreover, Gordobil *et al*. (2015) studied the effect of adding KL or acetylated KL mixed with PLA in terms of hydrophobicity and thermal stability.

Their results showed that PLA mixed with 5% acetylated KL enhanced the interaction between PLA and lignin, and it improved thermal stability by 17% relative to pure PLA. Thus, these polymer-lignin blends were able to better withstand temperatures used for extrusion.

To develop new value-added KL-based products, information on the thermal characteristics of KL, such as composition, thermal behavior, thermal stability, and pyrolysis products are necessary for future utilization of lignins. However, the majority of the information on KL has been focused on softwood KL. This study reports the thermal characterization of KL prepared from mixed hardwoods. KL was characterized by TGA (inert and oxidative conditions), DSC, and Py-GC/MS. The thermal characteristics of KL were compared alongside with milled wood lignins (MWLs) from acacia (MWL-aca) and mixed hardwoods (MWL-mhw) to gain insights on the structural changes that took place in KL during kraft pulping. Moreover, this study is an extension of previous works (Mun *et al*. 2021; Mun *et al*. 2022) on the characterization of KL produced in South Korea. The outcomes obtained in this study will aid the selection of chemical modifications, functionalization, and applications that are compatible with KL.

EXPERIMENTAL

Materials

The kraft lignin (KL) sample was kindly provided by Moorim P&P Co., Ltd. (Ulsan, Korea). The wood species used for kraft pulping were *Acacia* spp. from Vietnam and mixed hardwood (*Quercus* spp. + other hardwood, 1:1) from Korea. The ratio of these species present in KL was 50% acacia and 50% mixed hardwood. A detailed description about the cooking conditions and purification processes were described in an earlier work (Mun *et al*. 2021). Two milled wood lignins (MWLs) from *Acacia* spp. and mixed hardwood wood chips were prepared by fine ball milling and aqueous dioxane extraction method (Björkman 1954; Obst and Kirk 1988). Prior to thermal characterization, KL and MWLs were thoroughly dried in vacuum under P_2O_5.

Methods

Thermogravimetric analysis (TGA)

A 4 to 8 mg lignin sample was placed in a standard aluminum pan and secured in a thermogravimetric analyzer (Q600 SDT, TA Instruments). The samples were heated from 24 to 800 °C at 10 °C/min under nitrogen atmosphere. The lignin samples were also analyzed under oxidative atmosphere. TGA was performed at the Center for University-wide Research Facility (CURF), Jeonbuk National University (JBNU).

Differential scanning calorimetry (DSC)

A 2 to 6 mg lignin sample was loaded in a standard aluminum pan, and the heat flow was measured by a differential scanning calorimeter (DSC Q20, TA Instruments, New Castle, DE, USA). Each sample was heated from 40 to 240 °C at 10 °C/min under nitrogen atmosphere. The sample was cooled to 40 °C. The sample was again heated to 240 °C at the same heating rate. The glass transition temperature was estimated from the second heating cycle. DSC was performed at the CURF, JBNU.

Pyrolysis-gas chromatography/mass spectrometry (Py-GC/MS)

The lignin samples were derivatized using trimethylsilylation, which was adapted and slightly modified from the work of Kuroda (2000). A 1 mg lignin sample was dissolved in 100 µL pyridine (99.9%, Sigma-Aldrich, Schnelldorf, Germany) to disperse the lignin samples. Then, 100 µL of N,O-bis(trimethylsilyl)trifluoroacetamide/trimethylchlorosilane (99:1, Sigma-Aldrich) was added. The mixture was placed in a heating block at 55 °C for 30 min to complete silylation. About 60 µL of derivatized sample was enclosed in a pyrofoil (F670, Japan Analytical Industry Co., Ltd., Osaka, Japan) and placed in a quartz sample tube prior to pyrolysis. The derivatized sample was heated at 675 °C for 5 s using a Curie-point injector (JCI-21, Japan Analytical Industry Co., Ltd.). The pyrolysis products were introduced into a gas chromatograph/mass spectrometer (GCMS-QP2010 Ultra, Shimadzu, Kyoto, Japan) with helium as the carrier gas at a constant flow of 1 mL/min. The samples were injected in a 1:30 split ratio at an injection temperature of 280 °C. The resulting products were separated on a capillary column (30 m x 0.25 mm ID x 0.25 µm, Rxi-5MS, Shimadzu). The oven was programmed from 70 °C (held for 3 min) to 300 °C (held for 5 min) at a heating rate of 10 °C/min. The interface and ion source temperature were 230 °C and 200 °C, respectively. The pyrolysis products were ionized by electron impact method at 70 eV. The compounds were identified by comparing their mass spectra with published mass spectra from NIST and Wiley libraries (Faix *et al*. 1990; Ralph and Hatfield 1991). Py-GC/MS was performed at the CURF, JBNU.

RESULTS AND DISCUSSION

Thermogravimetric Analysis (TGA, Oxidative Condition)

TGA is a widely used technique for studying the composition, thermal behavior, and thermal and thermo-oxidative stability of lignins. Figures 1a and 1b show the thermogravimetric (TG) and derivative TG (DTG) curves of lignins under oxidative condition, respectively.

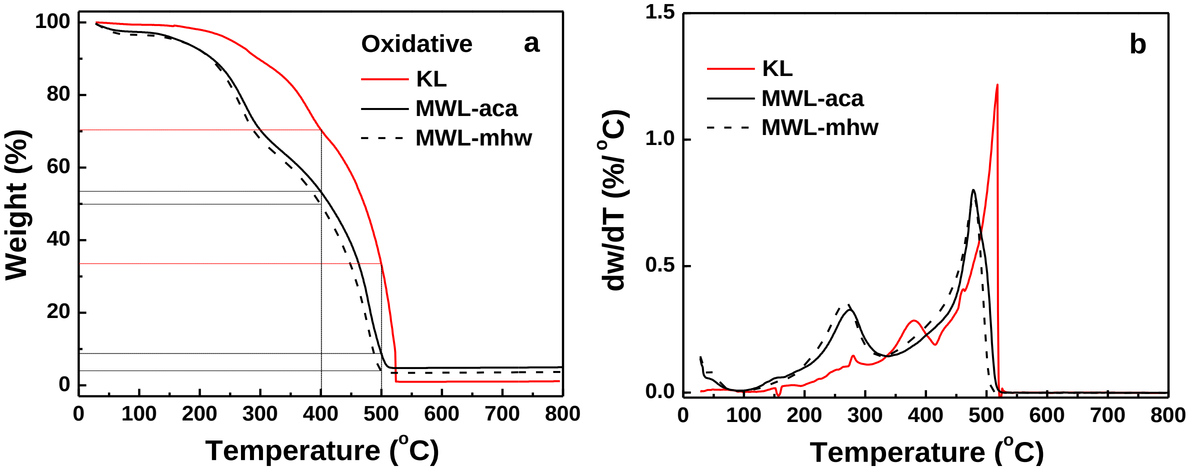

Fig. 1. a) TG and b) DTG curves of KL and MWLs under oxidative condition

In the TG curve, the temperature at which decomposition begins is known as the onset temperature. The onset temperature is an important indicator during thermal oxidation or pyrolysis experiments, since gases are started to be released during this temperature. Meanwhile, the maximum peak in the DTG curve (DTG_{max}) represents the temperature at which thermal degradation occurs at the fastest rate; hence, DTG_{max} is considered as a parameter for determining the thermal stability of lignins (Amit *et al*. 2021).

The TG curve (Fig. 1a) shows a distinction between the thermal profiles of KL and MWLs. The weight loss (volatiles) for KL and MWLs at 105 °C mainly corresponded to water bound to the lignin. In Table 1, the volatile content of KL was very low compared to that of MWLs, which suggests that KL is more hydrophobic than MWLs. The onset temperatures of KL and MWLs were relatively close around 220 °C. Compositional analysis at 400 °C shows that at least 70% residue remained in KL, while 50 to 53% residue remained in MWLs. At 500 °C, around 33% residue remained in KL compared to 4 to 9 % in MWLs. However, at 525 °C, KL showed a maximum weight loss which indicated rapid degradation of highly condensed aromatic structures. There were no weight changes beyond 550 °C. The near total degradation of KL (98.8%) and MWLs (~92.0%) at 800 °C was attributed to the accelerated degradation in the presence of air. Meanwhile, the ash content obtained at 800 °C from TG of KL (1.1%) was lower than that of MWLs (Table 1). This is because KL was prepared by acid precipitation from black liquor. Previously, the ash content was determined by the authors through ash analysis and was found to be 0.4%, lower than that of TG analysis.

The DTG curve (Fig. 1b) reveals the thermal behavior of lignin samples under oxidative conditions. KL (518 °C) had higher DTG_{max} than that of MWLs (~480 °C). This thermo-oxidative stability of KL is due to their condensed aromatic-rich contents. Moreover, when KL was oxidized, the site of oxidation was probably in the vicinity of the aromatic moieties rather than the aliphatic sidechains, considering that most of the sidechains were already cleaved. This caused the degradation of oxidized KL to be slightly more difficult than oxidized MWLs, since degradation of oxidized aromatic moieties needed more energy. Thus, the KL had higher DTG_{max} than that of MWLs.

Table 1. Composition, Onset Temperature, and DTG_{max} of Lignins (Oxidative)

	Composition (%)				Temperature (°C)	
Lignin	105 °C (Volatiles)	400 °C	500 °C	800 °C (Ash)	Onset	DTG_{max}
KL	0.1	70.4	33.3	1.1	228	518
MWL-aca	2.6	53.3	8.7	5.0	216	478
MWL-mhw	3.4	49.7	3.9	3.7	214	480

Thermogravimetric Analysis (TGA, Inert Condition)

The TG and DTG curves of lignins under inert condition are shown in Fig. 2. In the TG curve at 105 °C, a weight loss of 0.9% in KL and 3.1 to 3.7% in MWLs were noted (Table 2); this weight loss was due to absorbed water and low-molecular weight volatiles. The onset temperature was found to be 288 °C for KL, 226 °C for MWL-aca, and 212 °C for MWL-mhw. This suggests that the bond breaking processes, involving the removal of small molecular gases, were relatively easy in MWLs as compared to KL since MWLs have lower onset temperature. In contrast, KL required a higher temperature to start decomposition, since a majority of its linkages were of the condensed type.

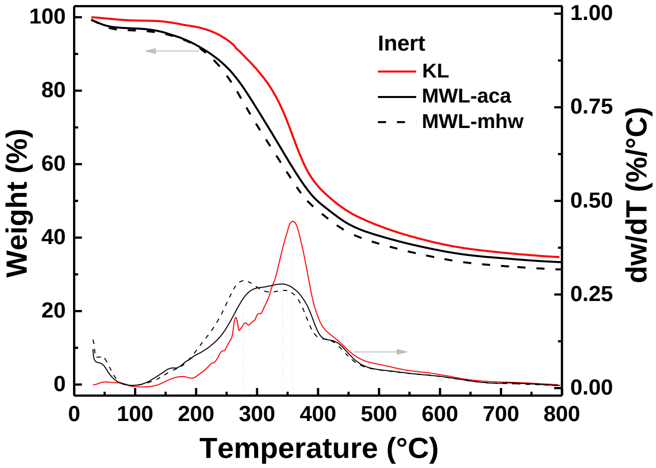

Fig. 2. TG and DTG curves of KL and MWLs under inert condition

In the DTG curve, there were two pyrolysis stages of interest: 225 to 300 °C and 325 to 375 °C. The first stage involved the release of gases such as water, carbon monoxide, carbon dioxide, and formaldehyde, which were generated from dehydration and decarboxylation reaction of aliphatic hydroxyl groups and carboxyl containing moieties in lignin. In addition, the ether (C–O–C) linkages were also broken at this temperature to yield monomeric phenols. Thus, for MWL-mhw, the peak at 276 °C represented the degradation of aliphatic side chains, specifically the scission of β-O-4 ether linkages. The second stage still released carbon monoxide and carbon dioxide, but it also included the gases methane and methanol. Most probably the formation of these gases was due to demethylation or demethoxylation of the aromatic ether linkages in lignin. For KL, the peak at 358 °C denoted the degradation of methoxyl groups. Information on the gases released during pyrolysis were based on the work of Liu *et al*. (2008) on birch hardwood lignin. A majority of the functional groups in lignin were decomposed at 460 °C and continuously carbonized at temperatures 600 to 800 °C. The residual content of KL at 800 °C was about 34.7%, which was 2 to 4% higher than that of MWLs.

Table 2. Composition, Onset Temperature, and DTG_{max} of Lignins (Inert)

	Composition (%)		Temperature (°C)	
Lignin	105 °C (Volatiles)	800 °C (Residue)	Onset	DTG_{max}
KL	0.9	34.7	288	358
MWL-aca	3.1	32.7	226	340
MWL-mhw	3.7	30.7	212	276

In terms of thermal stability, KL (358 °C) had higher DTG_{max} than that of MWLs (340 °C for aca and 276 °C for mhw), which indicates that KL is thermally more stable than MWLs. Higher thermal stability can be attributed to the formation of highly condensed aromatic structures (Tejado *et al*. 2007) and high carbon content in KL (Mun *et al*. 2021). Furthermore, the DTG_{max} obtained under inert condition (358 °C) was lower than the DTG_{max} obtained under oxidative conditions (518 °C). This is due to the difficulty of degrading oxidized condensed aromatic moieties. Thus, thermo-oxidation of KL can be potentially employed as a pre- or post-treatment for thermal applications requiring higher stability at higher temperatures.

Differential Scanning Calorimetry (DSC)

The thermal behavior of KL and MWLs in terms of heat flow as a function of temperature were determined in the range of 40 to 240 °C. The first heating, cooling, and second heating cycles of KL are shown in Fig. 3a. The heat-cool-heat cycles of MWLs were not shown but were analogous to KL. The first heating removes the thermal history (*i.e.*, moisture absorbed during storage conditions, residual solvents, and drying methods) of lignins. During the first heating, a characteristic endothermic peak at 110°C was due to the removal of physically adsorbed water. Upon reaching 240 °C, a temperature above their melting transition, each lignin sample was allowed to cool at 40 °C. An exothermic peak was evident in the cooling cycle, which indicates solidification of the lignin melt. After cooling, a second heating cycle was carried out to reveal the true thermal behavior of each lignin sample. The second heating curves of KL and MWLs, as compiled in Fig. 3b, shows a reliable estimate of the glass transition temperature (T_g), the temperature at which amorphous polymers change from glassy to rubbery state. T_g is influenced by the free volume between attractive forces between molecules, rotational freedom of molecular moieties, chain stiffness, chain length, and polymer chains (Glasser 1999). T_g is an important transition but polymers also exhibit other transitions such as softening temperature (T_s) (Irvine 1985). KL shows two thermal transitions, as shown in Fig. 1b, the first transition is the T_g and the second transition is the T_s.

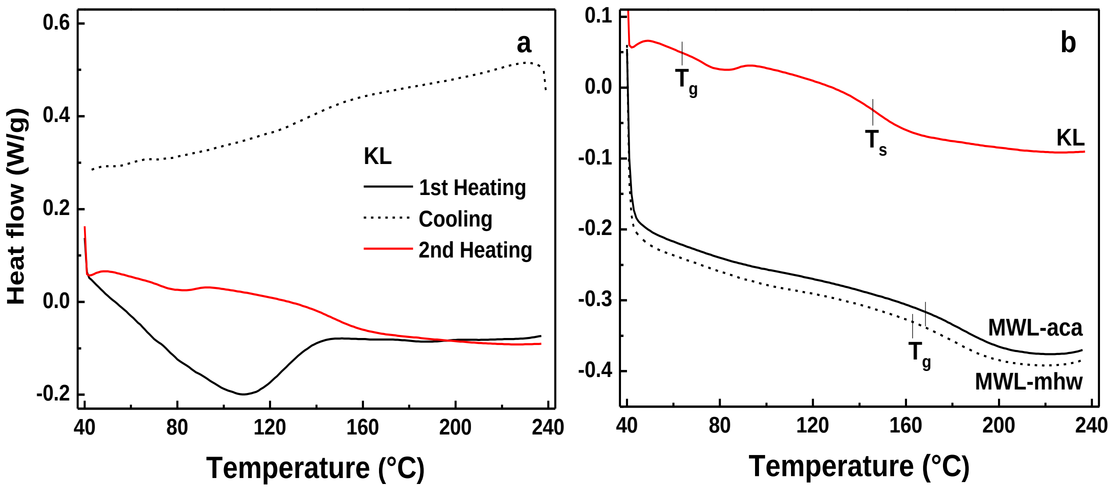

Fig. 3. a) DSC profile of KL and b) DSC second heating curves of KL and MWLs (exo up)

Table 3. Transition Temperatures of KL and MWLs

Lignin	T_g (°C)	T_s (°C)
KL	63.2	148.6
MWL-aca	167.3	-
MWL-mhw	162.3	-

As listed in Table 3, the T_g of KL was remarkably lower than MWLs, as the structure of KL was highly degraded. The weight average molecular weight (M_w) of KL was about 3,000 Da while MWLs were about 12,000 to 13,000 Da (Mun *et al*. 2021). In effect, there were lesser attractive forces in KL than MWLs, which led to a lower T_g value. The MWLs contained more attractive forces due to their high M_w, which explains the high

T_g values (162.3 to 167.3 °C). Analysis of the second heating cycle showed that KL had a second thermal transition at 148.6 °C, which was not evident during the first heating cycle.

Pyrolysis-Gas Chromatography/Mass spectrometry (Py-GC/MS)

Py-GC/MS was carried out at 675 °C to determine the composition of syringyl (S), guaiacyl (G), and *p*-hydroxyphenyl (H) groups present in the lignins. The selection of pyrolysis temperature was based on the TGA; wherein 675 °C was the chosen temperature since this had the least observable weight change in the DTG curve. About 30 monolignol compounds were identified during the pyrolysis at this temperature (Fig. 4). The pyrolysis products and their relative composition are listed in Table 4. The major pyrolysis products detected in KL were 4-methylphenol **2**, guaiacol **3**, 4-methylguaiacol **5**, 3-methoxycatechol **7**, 4-vinylguaiacol **9**, syringol **10**, 4-methylsyringol **15**, 4-vinylsyringol **21**, syringaldehyde **25**, and acetosyringone **27**. These 10 major pyrolysis products accounted for 57% of the total relative composition for KL. In terms of guaiacol **3** and syringol **10** contents, the most apparent pyrolysis products, the syringol content of KL was higher than its guaiacol content. However, in MWL-aca, guaiacol was about 2.5 times higher than syringol. This reveals that although *Acacia* spp. is a tropical hardwood, the species behaves as a temperate softwood due to its high guaiacyl content. In a recent work by Jardim *et al*. (2022), the pulping behavior of *Acacia* spp. was found to be similar to that of *Pinus* spp. In MWL-mhw, the guaiacol and syringol contents had a similar tendency with KL.

Interestingly, aromatic aldehydes such as vanillin **13** and syringaldehyde **25** had notably moderate amounts in MWLs; however, these were found to be reduced in KL. Similarly, the homovanillin **17** content was also lower in KL as compared to MWL-aca. In general, aldehydes are known to be unstable and reactive in highly alkaline conditions, especially during kraft pulping processes. Hence, the reduced amounts of these aldehydic components in KL.

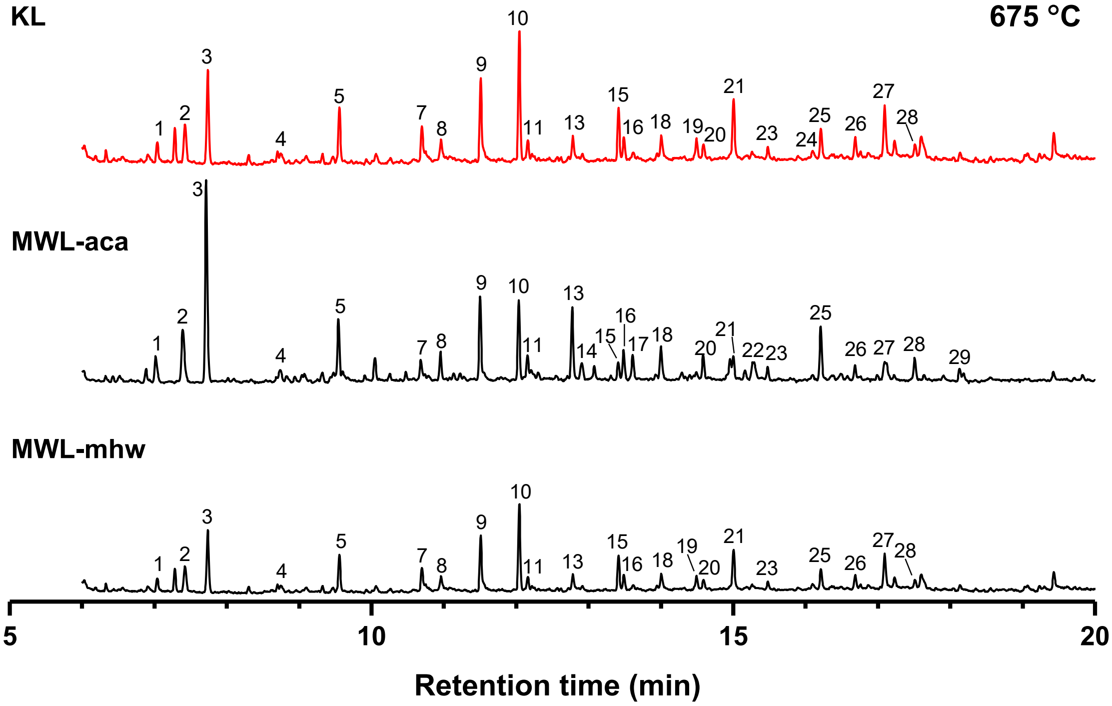

Fig. 4. Pyrograms of KL and MWLs at 675 °C

Table 4. Pyrolysis Products and Relative Composition at 675 °C

No.	Compound	RRT[a]	MW	*m*/*z*[b]	Relative Composition (%)		
					KL	aca	mhw
1	2-methylphenol	0.91	108	**108**, 77	2.5	2.6	2.0
2	4-methylphenol	0.96	108	**108**, 77	3.8	4.7	2.8
3	guaiacol	1.00	124	124, **109**, 81	7.7	16.7	7.6
4	2,4-dimethylphenol	1.13	122	**122**, 107	1.7	1.5	1.4
5	4-methylguaiacol	1.23	138	**138**, 123, 95	5.1	5.5	7.0
6	catechol	1.24	110	**110**, 64	1.2	1.4	1.3
7	3-methoxycatechol	1.38	140	**140**, 125, 97	3.7	2.3	3.3
8	4-ethylguaiacol	1.42	152	152, **137**	2.7	2.9	2.4
9	4-vinylguaiacol	1.49	150	**150**, 135	7.2	7.4	7.7
10	syringol	1.56	154	**154**, 139, 93	10.5	7.1	8.7
11	eugenol	1.57	164	**164**, 149, 131, 107, 77	2.7	2.6	2.2
12	4-propylguaiacol	1.59	166	**137**	1.3	1.3	1.3
13	vanillin	1.65	152	152, **151**	3.0	6.5	4.4
14	*(Z)*-isoeugenol	1.67	164	**164**, 149	1.7	2.0	1.7
15	4-methylsyringol	1.73	168	**168**, 153	5.0	2.1	6.1
16	(*E*)-isoeugenol	1.74	164	**164**, 149	2.9	3.1	3.6
17	homovanillin	1.76	166	166, **137**	1.8	2.7	1.6
18	acetovanillone	1.81	166	166, **151**, 123	3.0	3.4	3.0
19	4-ethylsyringol	1.88	182	182, **167**	2.8	1.3	2.0
20	guaiacylacetone	1.89	180	180, **137**	2.4	2.7	2.2
21	4-vinylsyringol	1.94	180	**180**, 165, 137	5.6	2.6	5.4
22	guaiacyl vinyl ketone	1.98	178	**178**, 151	1.9	2.1	1.5
23	4-allylsyringol	2.00	194	**194**, 91	2.2	1.7	2.6
24	(*Z*)-4-propenylsyringol	2.08	194	**194**	1.9	1.1	1.7
25	syringaldehyde	2.09	182	**182**, 181	3.5	5.0	5.3
26	(*E*)-4-propenylsyringol	2.16	194	**194**	2.9	1.8	3.8
27	acetosyringone	2.21	196	196, **181**	5.2	2.1	2.9
28	syringylacetone	2.26	210	**167**	2.4	2.4	2.8
29	propiosyringone	2.34	210	**181**	1.8	1.6	1.6

[a] RRT: relative retention time, guaiacol as the reference

[b] m/z values in bold: base peak; only m/z values > 30% of the base peak are included

Table 5 tallies the S:G:H composition found in Table 4. According to Py-GC/MS at 675 °C, the S/G ratio of KL was calculated as 1.07. The S/G ratio obtained from Py-GC/MS was in agreement with the S/G ratios obtained from ^{1}H NMR (1.13) and ^{31}P NMR spectroscopy (1.05) (Mun *et al*. 2021; Mun *et al*. 2022).

Table 5. S:G:H Composition and S/G Ratio of KL and MWLs

Lignin	% S	% G	% H	S/G
KL	47.5	44.5	8.0	1.07
MWL-aca	31.0	60.3	8.7	0.52
MWL-mhw	46.3	47.5	6.2	0.97

Figure 5 shows the possible degradation routes of major pyrolysis products from KL and MWLs. The most common moieties found in KL are stilbene, styrene, and diphenylmethane moieties (Gierer *et al*. 1964; Santos *et al*. 2013; Mun *et al*. 2022).

Stilbene moieties are thermally degraded into 4-vinylguaiacol **9** and 4-vinylsyringol **21** while styrene produces 4-methylguaiacol **5** and 4-methylsyringol **15**. Diphenylmethane moieties are degraded into guaiacol and syringol, and upon further demethylation, generates catechol **6** and 3-methoxycatechol **7**. In MWLs, β-O-4 linkages, comprising to about 60% in hardwood lignins, are predominantly cleaved to yield styrene-like structures; wherein, these structures undergo α-, β-, and γ-cleavage to yield similar pyrolysis products as mentioned above. Moreover, β-O-4 with α-carbonyl moieties give vanillin and syringaldehyde.

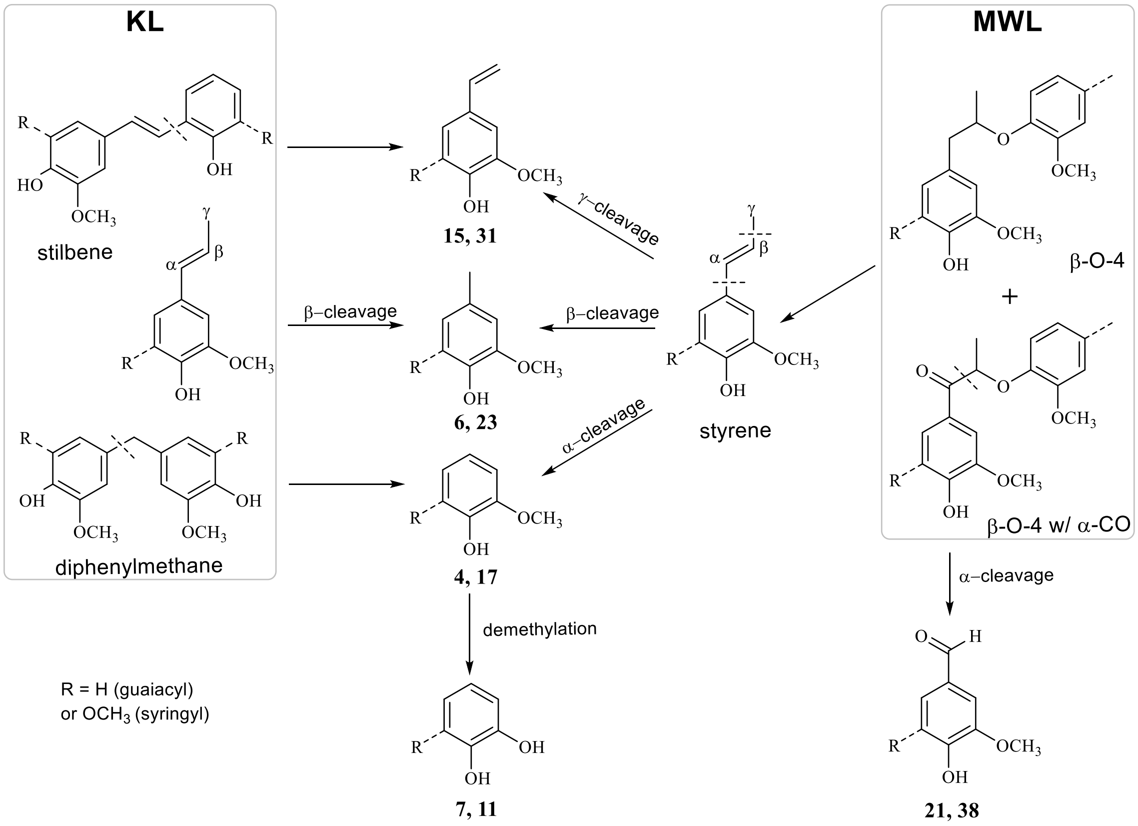

Fig. 5. Possible degradation routes of major pyrolysis products in KL and MWLs

CONCLUSIONS

1. Kraft lignin (KL) was found to have a higher maximum in differential thermogravimetry (DTG_{max}) than that of milled wood lignins (MWLs), whether in inert or oxidative conditions. Thus, KL exhibited better thermal and thermo-oxidative stability than MWLs. This thermal behavior of KL has potential to be employed for thermal applications requiring higher stability at higher temperatures.
2. The DSC glass transition temperature (T_g) of KL (63.2 °C) was lower than MWLs (162.3 to 167.3 °C). This lower T_g of KL can be explained by their corresponding molecular weight.

3. The major pyrolysis products of KL at 675 °C were 4-methylphenol, guaiacol, 4-methylguaiacol, 3-methoxycatechol, 4-vinylguaiacol, syringol, 4-methylsyringol, 4-vinylsyringol, syringaldehyde, and acetosyringone. A possible degradation route for these major products was proposed.
4. The S/G ratio of KL was 1.07, while MWL-aca and MWL-mhw were found to be 0.52 and 0.97, respectively. The S/G ratio of KL obtained from pyrolysis-GC/MS was in agreement with the S/G ratios estimated from ^{1}H NMR (1.13) and ^{31}P NMR (1.05).

ACKNOWLEDGMENTS

This research was supported by the National Research Foundation of Korea (NRF) grant funded by the Korean government (MSIT) (No. 2020R1A2C2012356). The authors are grateful to Moorim P&P, Co. Ltd. for providing the kraft lignin and wood chips (acacia and mixed hardwoods).

REFERENCES CITED

Amit, T. A., Roy, R., and Raynie, D. E. (2021). “Thermal and structural characterization of two commercially available technical lignins for high-value applications,” *Curr. Opin. Green Sustain. Chem.* 4, article 100106. DOI: 10.1016/j.crgsc.2021.100106

Bengtsson, A., Hecht, P., Sommertune, J., Ek, M., Sedin, M., and Sjöholm, E. (2020). “Carbon fibers from lignin-cellulose precursors: Effect of carbonization conditions,” *ACS Sustain. Chem. Eng.* 8(17), 6826-6833. DOI: 10.1021/acssuschemeng.0c01734

Björkman, A. (1954). “Isolation of lignin from finely divided wood with neutral solvents,” *Nature* 174, 1057-1058. DOI: 10.1038/1741057a0

Chen, F., Dai, H., Dong, X., Yang, J., and Zhong, M. (2011). “Physical properties of lignin-based polypropylene blends,” *Polym. Compos.* 32(7), 1019-1025. DOI: 10.1002/pc.21087

Demuner, I., Colodette, J. L., Demuner, A. J., and Jardim, C. (2019). “Biorefinery review: Wide-reaching products through kraft lignin,” *BioResources* 14(3), 7543-7581. DOI: 10.15376/biores.14.3.Demuner

Faix, O., Meier, D., and Fortmann, I. (1990). “Thermal degradation products of wood. A collection of electron-impact (EI) mass spectra of monomeric lignin derived products,” *Holz Roh Werkst* 48, 351-354. DOI: 10.1007/BF02639897

Gierer, J., Lenz, B., and Wallin, N. (1964). “The reactions of lignin during sulphate cooking. Part V. Model experiments on the splitting of aryl-alkyl ether linkages by 2N sodium hydroxide and by white liquor,” *Acta Chem. Scand.* 18(6), 1469-1476.

Glasser, W. G. (1999). “Classification of lignin according to chemical and molecular structure,” in: *Lignin: Historical, biological, and materials perspective*, W.G. Glasser *et al.* (eds.), ACS Symposium Series, vol. 742, Washington, DC. DOI: 10.1021/bk-2000-0742.ch009

Gordobil, O., Egüés, I., Llano-Ponte, R., and Labidi, J. (2014). “Physicochemical properties of PLA lignin blends,” *Polym. Degrad. Stab.* 108, 330-338. DOI: 10.1016/j.polymdegradstab.2014.01.002

Gordobil, O., Delucis, R., Egüés, I., and Labidi, J. (2015). "Kraft lignin as filler in PLA to improve ductility and thermal properties," *Ind. Crops Prod.* 72, 46-53. DOI: 10.1016/j.indcrop.2015.01.055

Irvine, G. M. (1985). "The significance of the glass transition temperature of lignin in thermomechanical pulping," *Wood Sci. Technol.* 19, 139-149. DOI: 10.1007/BF00353074

Jardim, J. M., Hart, P. W., Lucia, L. A., Jameel, H., and Chang, H. M. (2022). "The effect of the kraft pulping process, wood species, and pH on lignin recovery from black liquor," *Fibers* 10(16). DOI: 10.3390/fib10020016

Kadla, J. F., Kubo, S., Venditti, R. A., Gilbert, R. D., Compere, A. L., and Griffith, W. (2002). "Lignin-based carbon fibers for composite fiber applications," *Carbon* 40(15), 2913-2920. DOI: 10.1016/S0008-6223(02)00248

Kim, Y., Shim, J., Choi, J. W., Suh, D. J., Park, Y. K., Lee, U., Choi, J., and Ha, J. M. (2020). "Continuous-flow production of petroleum-replacing fuels from highly viscous kraft lignin pyrolysis oil using its hydrocracked oil as a solvent," *Energy Convers. Manag.* 213(1), 112728.

Kuroda, K. (2000). "Pyrolysis-trimethylsilylation analysis of lignin: preferential formation of cinnamyl alcohol derivatives," *J. Anal. Appl. Pyrolysis* 56(1), 79-87. DOI: 10.1016/S0165-2370(00)00085-1

Liu, Q., Wang, S., Zheng, Y., Luo, Z., and Cen, K. (2008). "Mechanism study of wood lignin pyrolysis by using TG–FTIR analysis," *J. Anal. Appl. Pyrolysis* 82(1), 170-177. DOI: 10.1016/j.jaap.2008.03.007

Mun, J. S., Pe, J. A., and Mun, S. P. (2021). "Chemical characterization of kraft lignin prepared from mixed hardwoods," *Molecules* 26(16), article 4861. DOI: 10.3390/molecules26164861

Mun, J. S., Pe, J. A., and Mun, S. P. (2022). "Characterization of kraft lignin prepared from mixed hardwoods by 2D HMQC and ^{31}P NMR analyses," *BioResources* 17(4), 6626-6637. DOI: 10.15376/biores.17.4.6626-6637

Obst, J. R., and Kirk, T. K. (1988). "Isolation of lignin," in: *Methods in Enzymology-Biomass. Part b, Lignin, Pectin, and Chitin*, Vol. 161, pp. 3-12. W.A. Wood and S. T. Kellogg (eds.), Academic Press Inc, San Diego, CA. DOI: 10.1016/0076-6879(88)61003-2

Ralph, J., and Hatfield, R. D. (1991). "Pyrolysis–GC–MS characterization of forage materials," *J. Agric. Food Chem* 39(8), 1426-1437. DOI: 10.1021/jf00008a014

Santos, R. B., Hart, P. W., Jameel, H., and Chang, H. (2013). "Wood based lignin reactions important to the biorefinery and pulp and paper industries," *BioResources* 8(1), 1456-1477. DOI: 10.15376/biores.8.1.1456-1477

Tejado, A., Peña, C., Labidi, J., Echeverria, J.M., and Mondragon, I. (2007). "Physico-chemical characterization of lignins from different sources for use in phenol–formaldehyde resin synthesis," *Bioresour. Technol.* 98(8), 1655-1663. DOI: 10.1016/j.biortech.2006.05.042

Article submitted: August 19, 2022; Peer review completed: October 9, 2022; Revised version received: October 18, 2022; Accepted: December 1, 2022; Published: December 6, 2022.
DOI: 10.15376/biores.18.1.926-936